IJST (2014) 38A1: 19-23
Iranian Journal of Science & Technology

http://ijsts.shirazu.ac.ir

The effect of TiO2 thin film on AC electrical properties of Nano porous silicon substrate

E. Khalili Dermani

Department of Physics, Kharazmi University, Tehran, Iran
E-mail: ensieh_khalili@yahoo.com

Abstract

The AC electrical behaviour of nano porous silicon (PSi) with TiO_2 thin films was examined over the range of frequency 10^2 to 10^5 Hz. Porous silicon (PSi) layers were obtained by electrochemical etching in HF solution and TiO_2 thin films were deposited on PSi substrates by using electron beam evaporation technique at room temperature. The porosity of PSi layer was found by using the gravimetric method and the crystalline properties of the TiO_2 thin films were obtained by an X-ray diffract meter. The surface morphology and AC electrical properties of samples were investigated by scanning electron microscopy (SEM) and electrometery respectively. For AC electrical properties we studied the dependence of capacitance and dissipation factor on frequency at different temperatures. The capacitance decreased with increasing frequency and increased with increasing temperature, and dissipation factor decreased with increasing frequency to a minimum value and after that increased. This behaviour is in good agreement with Goswami's theory. Also, the AC conductivity of sandwich structure films was studied over the range of frequency 10^2 to 10^5 Hz. Over the range of frequency$<10^3$Hz the band theory and over the range of frequency$>10^3$Hz hopping mechanism is applied in explaining the conductivity process.

Keywords: Porous Silicon; thin films; Sandwich devices; electrical conductivity; Goswami theory

1. Introduction

Porous silicon (PSi) has been investigated for various fields such as electronics, Nano electronic and optoelectronics because of its luminescence properties, high reactivity, large surface area and easy integratibility with the highly advanced Si technology (Makara et al., 2003; Vasquez-A et al., 2007; Ozdmir et al., 2007; Algun et al., 1999). PSi layers are composed of silicon wires and pores obtained by chemical or electrochemical etching of silicon wafers (Algun et al., 1990). The large surface area and the presence of a large number of unpaired dangling bonds alter the surface reactivity and stability of porous silicon (Bhagavannarayana et al., 2006). Unfortunately, many parameters of PSi layers often degrade with time, which leads to unstable working of PSi-based electronic devices. In recent years many efforts have been made to prepare of sandwich devices, which consist of PSi and thin films that can improve electrical and optical properties of PSi such as CdS, ZnO and ZnS (Zhao et al., 2010; Aroutiounian et al., 2009). In order to modify the properties of PSi for electronic and optoelectronic application the metal thin film such as TiO_2 can be used on the surface of PSi (Hasan et al., 2008). TiO_2 is a wide band gap n-type semiconductor (Hasan et al., 2008), with high refractive index and good chemical stability (Sung et al., 2007) which is used in many applications such as optical industrial (Yanget al., 2006), dye sensitized solar cells (Euvananon et al., 2008), dielectric applications (Tavares et al., 2007), gas sensors (Kim et al., 1998), self-cleaning purposes and biomedical fields (Mathews et al., 2009). A large number of investigations have been carryied out on electrical properties of porous silicon and TiO_2 thin film separately (Hwan et al., 2005; Stamate et al., 2005; Milani et al., 2006) but there is no work about AC electrical properties of porous silicon coated with TiO_2 thin film. In the present study we prepared PSi samples with electrochemical etching and TiO_2 thin films were deposited by electron beam gun evaporation technique on PSi samples and the AC electrical properties of TiO_2/PSi sandwich devices with Al electrode were investigated.

Received: 17 June 2013 / Accepted: 29 December 2013

2. Experimental

Monocrystal silicon substrates of p-type, B-doped, (100) orientation, resistivity of 0.5Ω-cm and thickness of about 525µm were cut into 1cm^2 square plates. The samples were immersed in the

HF aqueous solution to remove oxide from the silicon surface, and washed with RCA method.

In this cleaning method, the silicon wafer was immersed for 13 min in RCA solution (NH_4OH (29%): H_2O_2 (30%): H_2O) in a volume ratio of (1:1: 5) at a temperature of 80 °C. Then the wafer was immersed in (HCl (37%): H_2O_2(30%): H_2O) in a volume ratio of (1: 1: 6) at a temperature of 70 °C for 10 min and in the final step, the wafer was rinsed with DI water. An ohmic contact was obtained by evaporating a thin Al film with 50 nm thickness on the back side of the wafer by using thermal evaporation method under the vacuum of 10^{-5} mbar.

The porous silicon layers were obtained by anodization in (1:3:1) HF (%38): C_2H_5OH (%98): H_2O solution under a constant current density of 35mA/cm^2 for a duration of 20 minutes. Anodization was carried out with a platinum cathode. The porosity of samples was calculated via the following formula (Menna et al., 1995):

$$P = \frac{m_1 - m_2}{m_1 - m_3} \quad (1)$$

Where m_1 and m_2 are the masses of the samples before and after anodization process, respectively, and m_3 is the mass after dissolution of the porous layers in NaOH solution. The samples were then immersed in ethanol, dried in the air and placed in the electron beam evaporation chamber for deposition of the TiO_2 layers. Anatase TiO_2 metal oxide tablet target was used for electron beam evaporation. Thin films of TiO_2 with thickness of 42 nm were deposited on porous silicon under a vacuum of 10^{-5} mbar and deposition rate 0.6 nm per second. After the deposition process was completed, thin films were annealed at 500°C for 20 minutes. The TiO_2 thin films coated with Aluminum electrode as the metal were contact by using thermal evaporation method.

Figure 1 illustrates the XRD pattern of TiO_2 thin films obtained by an X-ray diffract meter (Equinox 3000) with wavelength of Cukα1 radiation. From the Fig., it was found that, the film was poly crystalline had anatase phase with lattice parameter a=0. 3785 nm matched well with that of the reference data. The (101) lattice plane diffraction peak was observed to have the highest intensity.

SEM image in Fig. 2 is shows the nano structure of PSi layer and the mean pore diameter is 37.50 nm. This image was taken via PhilipsXL30 scanning electron microscope. For AC electrical properties, the measurements were made by MT4080A LCR multifrequency meter over the frequency range of 10^2-10^5Hz in different temperatures.

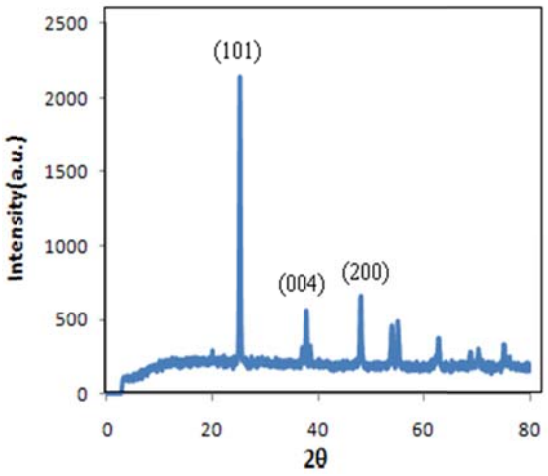

Fig. 1. XRD pattern of TiO2 thin film

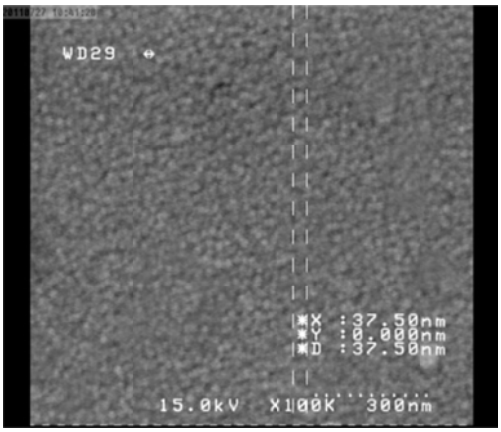

Fig. 2. SEM images from PSi samples with 20 minutes anodization time and 35mA/cm^2 current density

3. Result and discussion

3. 1. Capacitance and Dissipation Factor

The capacitance as a function of frequency in the frequency range 10^2 to 10^5 Hz was measured at temperatures 311, 335, 362 and 388 K. The diagram shows that, the variation of capacitance with frequency is intensive in high temperatures and low frequencies and this variation is less in low temperatures and high frequencies, but in general the capacitance decreased with increasing frequency. Also, the result shows increasing capacitance with increasing temperature. These results are more clearly shown in Fig. 2 and Fig. 3.

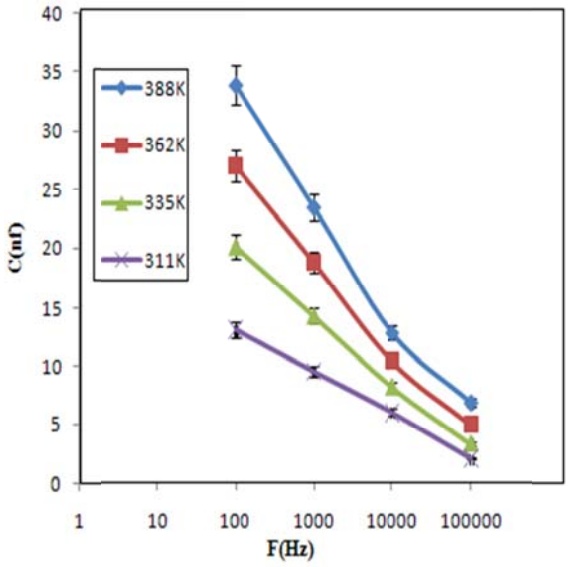

Fig. 3. Dependence of capacitance on frequency at different temperatures

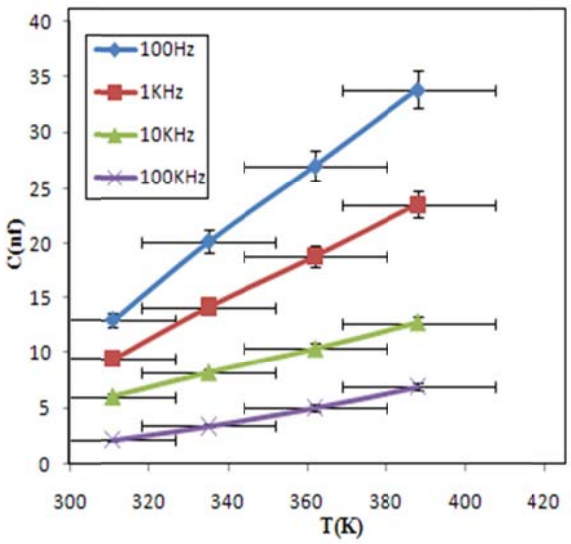

Fig. 4. Dependence of capacitance with temperature at different frequencies

A circuit model proposed by Goswami and Goswamican explains this type of behavior (Azimaraghi, 2007). In this theoretical model, the sandwich structure is modeled by an inferred capacity element (C) in parallel with a temperature dependent resistance R, both of which are in series with a resistance r due to lead length. The value of R is given by the equation: $R = R_0 \exp(\frac{\Delta E}{KT})$ where R_0 is a constant and ΔE is the activation energy.

Based on this model, the equivalent series circuit with a simple capacitance (C_s) is given by:

$$C_s = C + \frac{1}{\omega^2 R^2 C} \quad (2)$$

Where ω is the angular frequency. Equation (2) showed that, because of the decreasing value of R, C_s increased with increasing in temperature for any frequency. Also, this equation predicted that $C_s$decreased with increasing ω.

The dependence of dissipation factor (tanσ) with frequency and temperature is shown in Fig. 5. In general, dissipation factor decreased with increasing frequency, before passing through a minimum and then increased with increasing frequency again in higher frequencies. According to Goswami model, the dissipation factor is given by this relation:

$$\tan\sigma = \frac{1}{\omega RC}(1+\frac{r}{R}) + \omega rC \quad (3)$$

And the minimum value of ω is calculated by:

$$\omega_{\min} = \sqrt{\frac{1}{rRC^2}} \quad (4)$$

If we consider $\omega R^2 C \rangle\rangle r$ or $\frac{r}{R} \langle\langle 1$ we have:

$$\tan\sigma = \frac{1}{\omega RC} + \omega rC \quad (5)$$

In case of smaller ω, the second part of this equation becomes negligibly small and the equation is given by the first part, hence:

$$\tan\sigma = \frac{1}{\omega RC} \quad (6)$$

So dissipation factor decreases with increasing frequency at low frequencies.

From the large value of ω, $\frac{1}{\omega RC} \langle\langle \omega rC$ and then we have:

$$\tan\sigma = \omega rC \quad (7)$$

These results confirm increases in dissipation factor with increasing frequency at high frequencies.

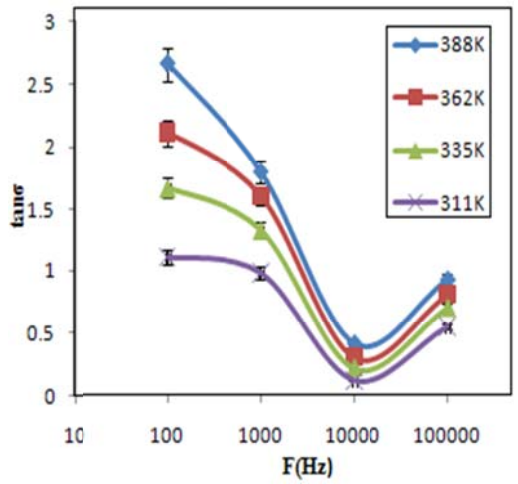

Fig. 5. Dependence of dissipation factor on frequency at different temperatures

3.2. AC Conductivity

The AC electrical conductivity calculated from this relation

$$\sigma_{AC}= \omega c \tan\sigma \quad (8)$$

Where ω is the angular frequency, C is the capacitance and tanσ is dissipation factor (Azimaraghi et al., 2010). The measurement is performed in the frequency range 10^2 to 10^5 Hz and temperature range 300 to 378 K. The result is shown in Fig. 6. The conductivity data exhibit strong frequency dependence. It was found that at low frequencies the conductivity decreases with increasing frequency at constant temperature, but in high frequencies the conductivity increases with increasing frequency. The conductivity of a semiconductor material can be expressed as:

$$\sigma=\sigma_{dc}+\sigma_{ac} \quad (9)$$

The first part is DC conductivity which is due to band conduction, and is frequency independent. The DC conductivity is important at low frequencies; such dependence may be described by variable range hopping (VRH) mechanism. The VRH model is frequency independent and only weakly temperature dependent compared to band theory and this model is important for electrical conduction mechanism (Panteny et al., 2005).

The second part of this relation is pure AC conductivity which is due to correlated barrier hopping (CBH) process (Yakuphanoglu et al., 2003). In general the relationship between AC conductivity and frequency is given by (Yakuphanoglu et al., 2003):

$$\sigma_{ac}=A\omega^S \quad (10)$$

Where A and S are characteristic parameters both of which depend on temperature, and the model based on correlated hopping of electrons over a barrier predicts a decrease in the value of the index S with the increase in temperature, and it was found to be consistent with the experimental results. The temperature dependence of the index S can be expressed as (Gould et al., 2003):

$$S=1-6KT/W_M \quad (11)$$

where W_M is the maximum high barrier. A decrease of W_M upon the temperature increase was observed. It can be seen that the value of S decreases with increasing temperature. Also, the index S can be determined from the slope of the lnσ-lnω curve (Gould et al., 2003).The values of S have been collected in Table. 1.

It has been observed that the conductivity is a decreasing function of frequency in the case of band conduction and an increasing function of frequency in the case of conductivity by hopping mechanism. Over the range of frequency < 10^3 Hz the band theory is applicable to explain the conduction process in Al/TiO_2/PSi/Al nano structures and in the range of frequency >10^3, the increasing of slope with increasing frequency connected with hopping conduction mechanism.

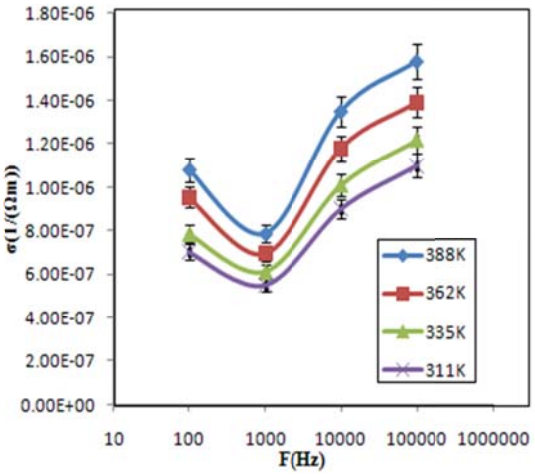

Fig. 6. Dependence of AC conductivity on frequency at different constant temperatures

Table 1. Dependence of the index S on temperature and frequency

Frequency range/Temperature	1000-10000Hz	10000-100000Hz
300K	0.152	0.253
316K	0.136	0.230
355K	0.107	0.217
378K	0.0899	0.213

4. Conclusion

Psi layers were prepared under a constant current density of 35mA/cm^2 for duration of 20 minutes and TiO_2 thin films were deposited with an EBPVD method on the surface of PSi layer. The porosity of PSi layers was found by using the gravimetric method and the main pore size of PSi layers was 37.50 nm. Dependence of capacitance and dissipation factor on the frequencyof different temperature was studied with an equivalent circuit model of Goswami and Goswami. Capacitance increased with increasing temperature and decreased with increasing frequency. Dissipation factor decreased with increasing frequency, before passing through a minimum and then increased with increasing frequency again in higher frequencies. We also studied the temperature dependence of the AC electrical conductivity in the Al/TiO_2/PSi/Al nanostructures. The result showed that over the range of frequency < 10^3 Hz the band theory and over the range of frequency>10^3 Hz the hopping mechanism with low power applied to explain the conduction process in Al/TiO_2/PSi/Al nanostructures.

References

Algun, G., Arikan, M, C. (1999). An investigation of electrical properties of porous silicon. Tr, J. of physics, 23, 789-797.

Aroutiounian, V., Arkelyan, V., Galstyan, V. (2009). Hydrogen sensor made of porous silicon and covered by TiO_{2-x} or ZnO(Al) thin film. Ieee. Sens. J, 9, 9.

Azimaraghi, M. E. (2007). Electrical properties of chloroaluminumphthalocyanine thin film sandwich devices. Ind. J. Pure Appl. Phys, 45, 40-43.

Azimaraghi, M. E., Abasi, S. (2010). AC electrical behavior of nanostructure thin film ClAlPc sandwich devices with aluminum electrode.J. Optoelectronics. Adv. Mater, 12, 1777-1780.

Bhagavannarayana, G., Sharma, S., Sharma, R. K., Lakshmikumar, S, T. (2006). A comparison of the properties of porous silicon formed on polished and textured (100) Si: High resolution XRD and PL studies. Mater. Chem. phys, 97, 442-447.

Euvananont, C., Junin, C., Inpor, K., Limthongkul, P., Thanachayanont, C. (2008). TiO_2 optical coating layers for self-cleaning applications. Ceram. Int, 34, 1067-1071.

Gould, R. D., Awan, S. A. (2003). Dielectric properties of RF-sputtered silicon nitride thin films with gold electrodes. Thin Solid Films, 433, 309-314.

Hasan, M. M., Haseeb, A. S. M. A., Saidur, R., Masjuki, H, H. (2008). Effect of annealing treatment on optical properties of Anatase TiO_2 thin films. Int. J. Chem. Biol. Eng, 1(2), 92.

Hwan an, M. (2005).Composition, structural and electrical investigations on DC- magnetron- sputtered TiO_2 thin films. J. Korean. Phys. Soc, 47, 847-851.

Kim, K. J., Kim, G. S., Hong, J. S., Kang, T. S., Kim, D. (1998). Characterization of a composite film prepared by deposition of TiO_2 on porous Si. Sol. Energy, 64, 61-66.

Lee, J., Han, W.,Ho Lee, J. (2011).Effect of ultrasonic on electrochemical Ai etching in porous Si layer transfer process for thin film solar cell fabrication.Sol. Eng. Mat. Sol. C, 95, 77-80.

Makara, V. M., Melnichenko, M. M., Svezhentsova, K. V., Khomenkova, L. Yu., Shmyryeva, O. M. (2003). Structure and luminescence study of nano porous silicon layers with high internal surface. Semiconductor Physics, Quantum Electronics & Optoelectronics, 6, 492.

Mathews, N. R., Morales, E., cortes-Jacome, A., Toledo Antonio, J. A. (2009). TiO_2thin films influence of annealing temperature on structural, optical and photocatalytic properties. Sol. Energy, 83, 1499-1508.

Milani, Sh, D., Dariani, R. S., Mortezaali, A., Dadmehr, V., Robbie, K. (2006). The correlation of morphology and surface resistance in porous silicon. J. Optoelectronics. Adv. Mater, 8, 1216-1220.

Menna, P., Di Francia, G., Ferrara, V-La. (1995). Porous silicon in solar cells: A review and a description of its application as an AR coating. Sol. Eng. Mat. Sol. c, 37, 13.

Ozdmir, S., Gole, L. (2007). The potential of porous silicon gas sensors. Curr. Opin. Solid. St. Mat, 11, 92.

Panteny, S., Stevens, R., Bowen, C. R. (2005). The frequency dependent permittivity and AC conductivity of random electrical networks.Tasylor& Francis, 319, 199-208.

Stamate, M.,Vascan, I., Lazer, I., Lazer, G., Caraman, I., Caraman, M. (2005). Optical and surface properties TiO_2 thin films deposited by DC magnetron sputtering method. J.Optoelectronics. Adv. Mater, 7, 771-774.

Sung, Y. M., Kim, H. J. (2007). Sputter deposition and surface treatment of TiO_2 films for dye-sensitized solar cells using reactive RF plasma. Thin Solid Films, 515, 4996-4999.

Tavares, C. J., Vieira, J., Rebouta, L., Hungerford, G., Coutinho, P., Teixeira, V., Carneiro, J, O., Fernandes, A. J. (2007). Reactive sputtering deposition of photo catalytic TiO_2 thin films on glass substrates. Mater. Sci. Eng, 138, 139-143.

Vasquez, A. M. A., Aguila Rodriguez, G., Garcia-Salgado, G., Romero-Paredes, G., Pena-Sierra, R. (2007). FTIR and photoluminescence studies of porous silicon layers oxidized in controlled water vapor conditions. Rev. Mex. Fis, 53, 431.

Yakuphanoglu, F., Aydogdu, Y., Schatzschneider, U., Rentschler, E. (2003). DC and AC conductivity and dielectric properties of the metal-radical compound: Aqua[bis(2-dimethylaminomethyl-4-NIT-phenolato)]copper(II). Solid State. Commun, 128/2-3, 63-67.

Yang, W., Wolden, C. A. (2006). Plasma-enhanced chemical vapor deposition of TiO< sub> 2</sub> thin films for dielectric applications. Thin Solid Films, 515, 1708-1713.

Zhao, Y., Lv, Z., Wang, L., Min, J., Shia, W., Lu, X. (2010). The effect of Al and B on the luminescent property of porous silicon. Curr. Appl. Phys, 10, 930.